Effect of quenched and correlated disorder on growth phenomena

Kent Bækgaard Lauritsen,* Muhammad Sahimi,† and Hans J. Herrmann
HLRZ Supercomputer Center, c/o Kernforschungsanlage Jülich, W-5170 Jülich 1, Germany
(Received 21 October 1992; revised manuscript received 23 February 1993)

We investigate the effect of quenched disorder with long-range correlations on two growth phenomena, namely, diffusion-limited aggregation (DLA) and the dielectric-breakdown model (DBM). The motivation for this study arises from experimental observations indicating that the permeability and hydraulic conductivity of heterogeneous rock masses seem to follow a fractional Brownian motion (FBM), a distribution that induces correlations that are essentially of infinite extent. A two-dimensional FBM is used to generate the conductivities of the medium in which DLA and DBM clusters are grown. A cutoff is also introduced into FBM that allows one to tune the length scale over which the conductivities are correlated. The results indicate that long-range correlations play a dominant role in the growth of the clusters, and the effect of all other factors, which could be important if there were no long-range correlations, is negligible. The results are completely different from those of disordered but uncorrelated media, and also reveal large differences between the DBM and DLA models. Thus any realistic modeling of transport in heterogeneous rocks must take into account the effect of such correlations.

PACS number(s): 68.70.+w, 47.55.Mh

I. INTRODUCTION

In recent years fractal and nonequilibrium growth processes have attracted much attention [1–4] due to their relevance to a wide variety of phenomena such as coagulation of colloidal particles, displacement of one fluid by another, growth of tumors, mechanical and electrical breakdown of disordered materials, electrochemical deposition, and turbulence. A wide variety of models for describing such phenomena have been proposed and studied by analytical and numerical methods, and several experimental studies have confirmed their validity.

Most of the structures that are generated by growth processes are disordered, and much of the recent advances in understanding such phenomena are due to the fact that these disordered structures exhibit scaling in both time and space. As a result, most of the recent studies have focused on investigating the scaling properties of such structures and the associated critical exponents. However, these studies are based on the assumption that the disorder in the structure of the systems formed by growth processes arises from the stochastic noise having short-range correlations in space and/or time. In practice, there are many systems in which the stochastic noise or disorder is quenched into the system with long-range correlations between various regions of the system. For example, natural rock masses may be characterized [5–7] by spatially varying permeabilities or hydraulic conductivities with long-range correlations (see below). As a result, flow and transport in natural rocks can be greatly influenced by such correlations. Although there have been several recent studies of the effect of long-range correlations on growth phenomena [8–12], they have been restricted to deposition processes in which it is only the surface of the system that exhibits interesting and nontrivial behavior, and the bulk of the system is compact. Moreover, these studied were restricted either to the case of one-dimensional spatial correlations, or to correlations in time only.

The purpose of this paper is to undertake a systematic study of the effect of quenched disorder with long-range correlations on two typical growth processes, namely, the diffusion-limited aggregation (DLA) model [13] and the dielectric-breakdown model (DBM) [14] in a two-dimensional system. The type of quenched disorder that we use is motivated by the statistical distributions that have been shown to describe the hydraulic conductivities of macroscopically heterogeneous rocks [5–7]. Moreover, changing a single parameter in the distribution allows us to obtain a variety of interesting growth patterns.

The plan of this paper is as follows. In the next section we describe the disorder distribution that we use and its properties, the motivation for using such a distribution, and how it is used in the models. Next we describe briefly the two models that we study in this paper. We then present and discuss the results.

II. GENERATION OF QUENCHED DISORDER WITH LONG-RANGE CORRELATIONS

There are many different methods for generating quenched disorder. However, generation of disorder with long-range correlations is not straightforward. One of the most useful models for doing this is the *fractional Brownian motion* (FBM) due to Mandelbrot and Van Ness [15]. Consider a stationary stochastic process $B_H(x)$ with the following mean and variance:

$$\langle B_H(x)-B_H(x_0)\rangle=0\ , \tag{1}$$

$$\langle [B_H(x)-B_H(x_0)]^2\rangle \sim |x-x_0|^{2H}\ , \tag{2}$$

where x and x_0 are two arbitrary points, and H is called the Hurst exponent [15]. The usual Brownian motion or random walk corresponds to $H=\frac{1}{2}$. A remarkable prop-

erty of this function is that it generates correlations whose extent is essentially infinite. For example, if a correlation function is defined by [16,17]

$$C(x)=\frac{\langle -B_H(-x)B_H(x)\rangle}{\langle B_H(x)^2\rangle}\ , \tag{3}$$

then one finds that $C(x)=2^{2H-1}-1$, i.e., the correlation function is *independent* of x. Moreover, the type of correlations can be tuned by varying H. If $H>\frac{1}{2}$, then FBM displays *persistence*, i.e., a trend (a high or low value of the variable) at x is likely to be followed by a similar trend at $x+\Delta x$. On the other hand, if $H<\frac{1}{2}$, then FBM generates *antipersistence*, i.e., a trend at x is not likely to be followed by a similar trend at $x+\Delta x$. For $H=\frac{1}{2}$, there are no correlations of the type defined above, and the overall shape of FBM traces is similar to ordinary random walks. Thus, varying H allows us to generate highly correlated or anticorrelated quenched disorder. This one-dimensional distribution can be easily extended to higher dimensions. One now writes

$$\langle [B_H(\mathbf{r})-B_H(\mathbf{r}_0)]^2\rangle \sim |\mathbf{r}-\mathbf{r}_0|^{2H}\ , \tag{4}$$

where $\mathbf{r}=(x,y,z)$, and $\mathbf{r}_0=(x_0,y_0,z_0)$.

A convenient way of representing a distribution function is through its spectral density $S(\mathbf{f})$, which is the Fourier transform of its variance. For FBM in d dimensions it can be shown [16] that

$$S(\mathbf{f})\sim\frac{1}{\left[\sum_{i=1}^{d} f_i^2\right]^{H+d/2}}\ , \tag{5}$$

where $\mathbf{f}=(f_1,\ldots,f_d)$. We may also introduce a cutoff a such that

$$S(\mathbf{f})\sim\frac{1}{\left[a+\sum_{i=1}^{d} f_i^2\right]^{H+d/2}}\ . \tag{6}$$

Introducing this cutoff allows us to control the length scale over which the heterogeneities are correlated (or anticorrelated). Thus, for length scales $l<1/a^{1/2}$ they preserve their correlations (anticorrelations), but for $l>1/a^{1/2}$ they become random and uncorrelated. The spectral density representation of the distribution also provides a convenient method for generating a sequence of numbers that obey a FBM. One first generates random numbers, uniformly distributed in (0,1), and assigns them to the sites or bonds of a d-dimensional lattice. One then calculates the Fourier transform of the d-dimensional array of the random numbers (knowing the distance between any two numbers on the lattice). The Fourier transformed numbers are then multiplied by a factor which is the square root of the right-hand side of Eq. (5) or (6). The resulting numbers are then inverse Fourier transformed back into the real space. The numbers so obtained follow a FBM. More details about the method are given elsewhere [17]. To avoid the problems associated with periodicity that arises from Fourier transforming of the numbers assigned to the lattice sites or bonds, one can generate the numbers for a large lattice, and use only a portion of it. Figure 1 presents the numbers generated by a two-dimensional FBM with $H=0.8$ and three values of the cutoff a. In order to generate these numbers a 2000×2000 square lattice was used, and the numbers shown correspond to a 1000×1000 portion of the lattice. In all cases the same initial sequence of random numbers was used for Fourier transforming, and thus the difference between the various cases is only due to the nature of FBM. Note that since $H=0.8>0.5$, the numbers are positively correlated, and therefore for $a=0$ the curve is relatively smooth. However, as can be seen, the cutoff generates randomness at large scales, although at smaller scales the correlations are preserved [Figs. 1(b) and 1(c)]. For larger values of the cutoff [Fig. 1(c)] the

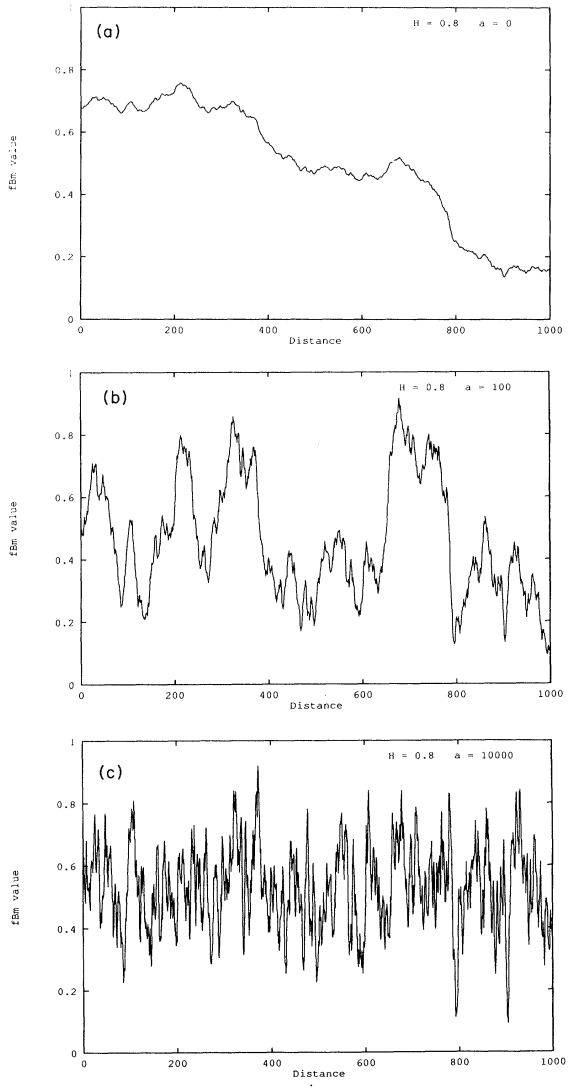

FIG. 1. The distribution of the numbers generated by a two-dimensional FBM with $H=0.8$ and various values of the cutoff a. (a) $a=0$ corresponds to numbers that are infinitely correlated. In (b) and (c) the numbers are not correlated for distances $l>1/a^{1/2}$. Distances are measured in units of lattice bonds.

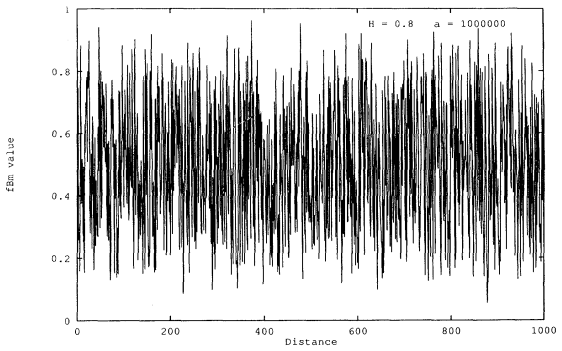

FIG. 2. The distribution of the numbers generated by a two-dimensional FBM with $H=0.8$ and $a=10^6$. In this case the numbers are correlated only for $l<10^{-3}$.

distribution seems to be different from that shown in Fig. 1(a), because for such values only small-scale structure of the distribution without the cutoff is preserved. Moreover, for very large values of the cutoff (Fig. 2) there is a transition from the correlated (or anticorrelated if $H<0.5$) structures to Gaussian or white noise, corresponding to $H=-\frac{1}{2}$. White noise so obtained is the derivative of the trace of Brownian motion ($H=\frac{1}{2}$) and, therefore, corresponds to $H=-\frac{1}{2}$. Figure 3 shows the results for $H=0.2$, i.e., the case in which the numbers are anticorrelated. The same initial sequence of random numbers as that of Figs. 1 and 2 was used for Fourier transforming and generating the results. For $H<0.5$, one has antipersistent patterns, namely, a large number is likely to be followed by a small one and vice versa and, as a result, the distribution is very rough, which Fig. 3(a) demonstrates nicely. Increasing the cutoff a only increases the roughness, and thus the distribution will look even more random [Figs. 3(b) and 3(c)].

In this paper, we use such two-dimensional FBMs for generating quenched disorder. The motivation for doing this is that extensive experimental studies of macroscopically heterogeneous reservoir rocks [5–7] have shown that their hydraulic conductivity follows a FBM with $H\simeq 0.7-0.8$. Moreover, the analysis of large-scale heterogeneities of rocks, e.g., fractures and faults, have indicated [18,19] that the fracture and fault patterns are closely related to a FBM. Therefore, we study the effect of quenched and correlated disorder represented by a FBM on growth phenomena governed by the DBM and DLA models. Since it has already been established that [7,20] the DBM and DLA model can reproduce certain features of displacement of one fluid by another in a porous medium, our study is directly relevant to transport and displacement processes in *large-scale and macroscopically heterogeneous rocks*. Thus, we assign the hydraulic conductivities of a porous medium from a FBM, and study how the growth patterns evolve in a medium with quenched and correlated disorder.

III. DLA AND DBM IN A MEDIUM WITH QUENCHED AND CORRELATED DISORDER

We have investigated the DBM and DLA model in a macroscopically heterogeneous porous medium represented by a square network. Each bond of the network is assumed to represent a portion of the medium over which it is homogeneous. However, since we are interested in macroscopically heterogeneous porous media, the hydraulic conductivity of the bonds must vary spatially with long-range correlation. Therefore, we use a two-dimensional FBM to generate the conductivities. Both DLA and the DBM can be simulated by random-walk methods, or by directly solving the Laplace equation on the network; we have used the latter method. Thus, in both models one solves the discrete Laplace equation on a lattice with quenched disorder,

$$-(\Delta\phi_i)=\sum_j(\phi_i-\phi_j)\sigma_{ij} \ , \tag{7}$$

where ϕ_i is the potential at site i of the lattice, σ_{ij} is the

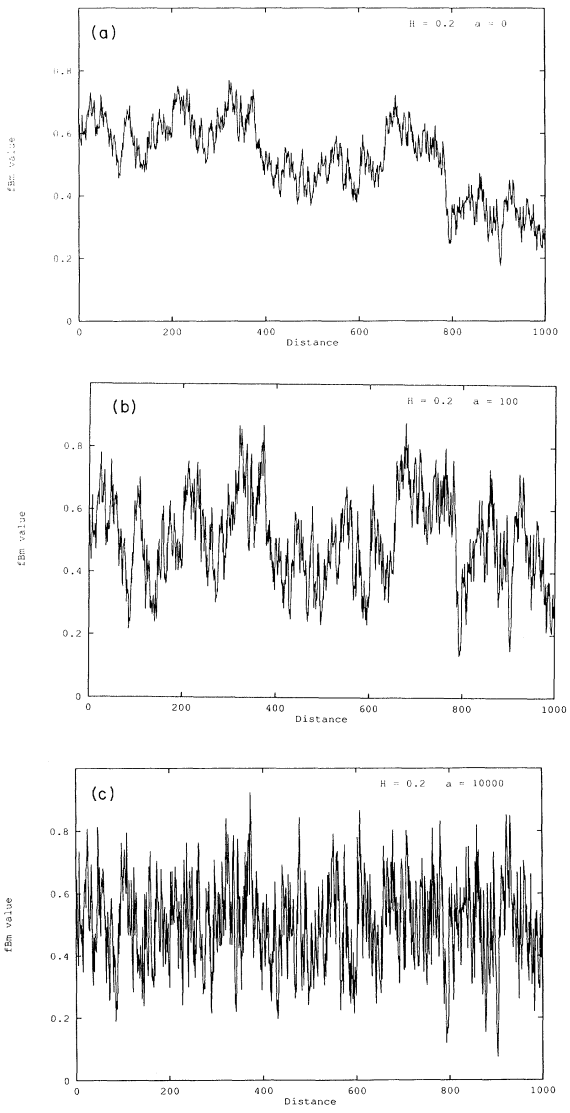

FIG. 3. The distribution of the numbers generated by a two-dimensional FBM with $H=0.2$ and various values of the cutoff a. In (a) the numbers are anticorrelated at all scales, whereas in (b) and (c) they are anticorrelated only for $l>1/a^{1/2}$.

conductivity of the bond between i and j, and the sum is over all nearest neighbors j of i. We assume that the conductivities are distributed according to FBM, and thus are highly correlated, or anticorrelated, depending on the value of H. In both models one boundary condition is that far from the growing cluster, $\phi=1$. The difference between the two models is in the boundary condition at the front (interface) separating the growing cluster from the empty sites of the network. While in the DBM $\phi=0$ on the interface sites of the cluster, in the DLA model $\phi=0$ on the empty sites adjacent to the interface. It is also well known that the shape of the clusters in both models is very sensitive to noise and fluctuations that are the result of the random growth of the clusters. Therefore, in order to eliminate the effect of this randomness and study only the effect of quenched disorder represented by the distribution of the conductivities, we used DLA and the DBM in the limit of infinite noise reduction [21–23]. In this limit, one assigns counters c_i to the bonds or sites of the lattice which take on zero values at the beginning of the simulation. At each stage of the simulation the values of the counters are updated according to

$$c_i \rightarrow c_i + \alpha \nabla \phi \ , \tag{8}$$

where α is the minimum of $(1-c_i)/\nabla\phi$, and $\nabla\phi$ is potential gradient at the counter's site or bond. Thus, the site or bond for which the value of the counter reaches unity is added to the growing cluster, the boundary condition at, or adjacent to, the interface is modified, the Laplace equation is solved again, and so on. Moukarzel [24] and Batchelor and Henry [25] studied DLA and the DBM in the limit of zero noise. However, no quenched disorder of the type that is of interest to us was present in their simulations.

In the DLA model we put the counters on the bonds of the lattice, whereas in the DBM the counters are associated with the sites. The idea is that simulation of DLA or the DBM in a disordered lattice may correspond to a miscible or an immiscible displacement process in a porous medium, where the bonds and sites of the lattice represent, respectively, the pore throats and pore bodies of the medium. In the DLA case, it is assumed that the pore throats control the displacement process, and the pore bodies are neglected, whereas it is the opposite case in the DBM case. Such assumptions about the role of pore bodies or pore throats have been used by many authors in the past, and our work allows us to check their effect on the growing patterns in the presence of quenched disorder with long-range disorder. Moukarzel [24] has already investigated four distinct cases, namely, when the counters are put on the bonds or sites of the lattice in both the DBM and DLA model. However, Moukarzel was interested in the effect of the random topology of a lattice on the growth patterns, and thus investigated these models on a variety of topologically disordered lattices; the effect of quenched disorder on the values of conductivities with correlations was not studied.

We first generated the random conductivities according to the FBM described above and assigned them to the bonds of the lattice. In all cases, we used 2000×2000 lattices, and then used a 200×200 portion of them for growing the clusters. For all values of H the same initial sequence of random numbers was used for the initial Fourier transforming and generating the conductivities, and therefore the difference between the distribution of the conductivities for various values of H is due to the nature of FBM, and has nothing to do with the inherent noise in the initial frequency of the random numbers. The Laplace equation was solved by the conjugate-gradient method, using a fully vectorized algorithm developed by Moukarzel [24]. All computations were carried out on a Cray-YMP supercomputer. No attempt was made to determine the fractal properties of the clusters, if any, since we are only interested in the effect of quenched disorder with long-range correlation on the shape of the clusters. Moreover, the computations, including the generation of the conductivities according to FBM, are very intensive and time consuming, and generation of very large clusters for estimating their fractal properties requires very large amounts of CPU time.

IV. RESULTS AND DISCUSSION

Figure 4 presents the results of our simulations for the DBM for various values of H. The case $H=-0.5$ corresponds to white noise (completely random numbers). Even in this case, thick branches form and, moreover, a lot of tip splitting occurs which is undoubtedly due to the random but uncorrelated distribution of the conductivities. As H is increased to zero, the branches become thicker and tip splitting appears to reduce. For $0<H<0.5$ the values of the conductivities are anticorrelated, and therefore it is likely that a bond with a large conductivity is followed by a low-conductivity bond and vice versa. This implies that the path of the growing cluster is still very heterogeneous, and therefore tip splitting may still be expected to occur and, indeed, the patterns for $H=0$ and $H=0.2$ confirm this. For $H=0.5$ the trace of FBM is that of a random walk, but there are correlations in the system, and for $H>0.5$ the conductivities become positively correlated, and thus in some sense the medium is less disordered and we may expect tip splitting to decrease. Indeed, as Fig. 4 indicates, with increasing H the number of branches and the amount of

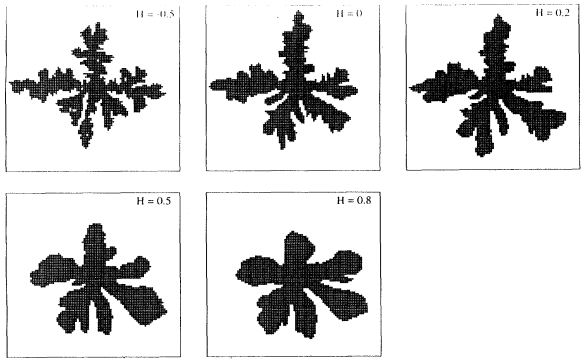

FIG. 4. Growth patterns as a function of H obtained with the DBM.

tip splitting decrease significantly.

In Fig. 5 we show the effect of the cutoff on the patterns grown with the DBM for $H=0.8$. As the cutoff increases, the length scale over which the conductivities are correlated decreases, and therefore for a fixed H the amount of disorder should increase (see Figs. 1 and 2) at large scales. Thus, we expect the growing cluster to take on an increasingly random shape, and Fig. 5 confirms this trend. Figure 6 shows the effect of the cutoff for $H=0.2$, i.e., the anticorrelated case. Since $H<0.5$ gives rise to a highly disordered system with anticorrelations (Fig. 3), and because the cutoff decreases the size of the region in which the conductivities are correlated or anticorrelated, compared with Fig. 5, we expect to see more disordered patterns, and Fig. 6 confirms this. However, since for very large values of the cutoff a, and regardless of the value of H, FBM approaches a white noise, the shapes of the clusters for both $H=0.8$ and 0.2 should be essentially the same for $a=10^6$ and be similar to the case $H=-0.5$, and Figs. 5 and 6 also confirm this expectation.

Figure 7 presents the results for the DLA model and shows patterns which are completely different from those for the DBM. Thick branches are not formed with the DLA model, because they are due to the inherent surface tension effect that is present in the DBM but not in DLA. Surface tension acts as a stabilizing agent, and thus the clusters tend to be compact. Such an effect is absent in DLA, and therefore one finds a more open and random structure in DLA clusters. As H increases, the DLA clusters take on an increasingly dendritic (ordered) structure. For $H>0.5$ the conductivities are positively correlated, and therefore the bond-to-bond variations of the conductivities are not large, and hence the shape of the cluster is somewhat similar to that in an ordered porous medium without any correlations. This expectation is confirmed by experiments in which a fluid displaced a much more viscous and miscible fluid in an ordered porous medium [26]. However, Fig. 7 (and 4) also tells us that in modeling transport and displacement in porous media, it is not enough to include only pore-level heterogeneities without any correlations, because then we would only obtain random and very open (fractal-like) structures for DLA and DBM clusters, whereas long-range correlations, which are presumably present in natural rocks, give rise to completely different patterns. Thus, if we do not take into account the effect of long-range correlations, our predictions for various properties of transport and displacement processes in natural rocks could be in error (see below). Note that in the limit $H=-\frac{1}{2}$ the structure of the cluster is still random to some extent, even though it is generated in the limit of zero noise.

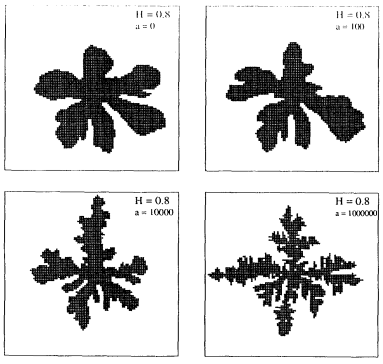

FIG. 5. The effect of the cutoff a on the growth patterns obtained with the DBM. $H>0.5$ indicates that the conductivities are correlated.

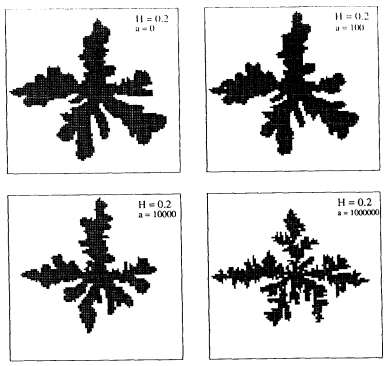

FIG. 6. The effect of the cutoff a on the growth patterns obtained with the DBM. $H<0.5$ indicates that the conductivities are anticorrelated.

In Fig. 8 the effect of the cutoff on the DLA clusters for $H=0.8$ is shown. The effect of a is to some extent similar to that for the DBM (Fig. 5), namely, as the cutoff increases, the length scale over which the conductivities are correlated decreases, and therefore beyond a certain length scale l defined above, the conductivities are essentially random and uncorrelated. Therefore, at large length scales, the clusters should take on random structures, and Fig. 8 confirms this. Figure 9 presents the effect of the cutoff for $H=0.2$, and again the trends are similar to those of the DBM.

To quantify the difference between the various patterns, we calculated the *sweep efficiency* of each system, i.e., the fraction of the sites of the original system occupied by the aggregate. This quantity is routinely used in the oil industry for characterizing the efficiency of a dis-

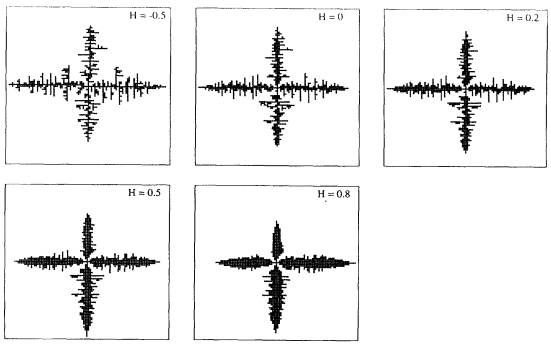

FIG. 7. Growth patterns as a function of H obtained with the DLA model.

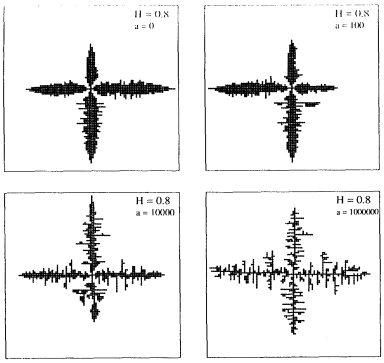

FIG. 8. The effect of the cutoff a on the growth patterns obtained with the DLA model, if the conductivities are correlated.

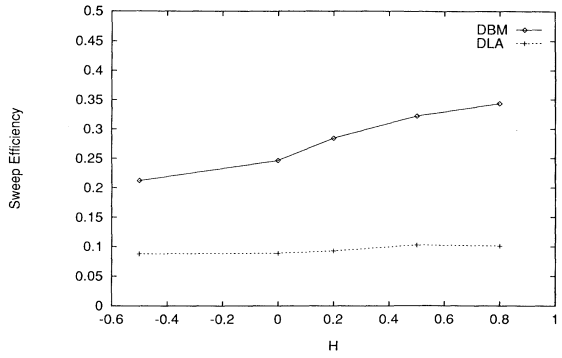

FIG. 10. The effect of H, the parameter of the FBM, on the sweep efficiency of the DBM and DLA model. The cutoff is $a=0$.

placement process. Figure 10 shows the dependence on H of the sweep efficiency for both the DBM and DLA model with $a=0$. It may seem surprising that for the DLA model H has virtually no effect on the sweep efficiency. However, Figs. 7–9 reveal the DLA patterns do not change much as H is varied. In contrast, the sweep efficiency in the DBM increases by a factor of about 2 as H is increased from -0.5 to 0.8. Although this increase may also seem unexpected, Figs. 4–6 tell us that as H increases the branches of the aggregates become thicker, thereby increasing the sweep efficiency of the process. Another notable feature of Fig. 10 is the large difference between the sweep efficiency of the two models. In the literature [1], the DBM and DLA model have been considered as essentially equivalent. However, Fig. 10 tells us that, e.g., at $H=0.8$ (which is the value that seems to describe the distribution of permeability of heterogeneous rocks) the sweep efficiency of the DBM is about 7 times larger than that of the DLA model. Thus, one model cannot be used for simulating the other. A glance at the literature indicates that the DBM has been used frequently for modeling miscible displacement processes, because of the belief that it is essentially equivalent to the DLA model. We remind the reader that the DLA model corresponds to a miscible displacement in which an inviscid fluid displaces a viscous one [20].

Figure 11 presents the effect of the cutoff a on the sweep efficiency of the two models. As in Fig. 10, the cutoff has virtually no effect on the sweep efficiency of the DLA model, whereas it has a rather large effect on the efficiency of the DBM. Moreover, as a increases, i.e., as the length scale $l=1/a^{1/2}$, over which the conductivities and permeabilities are correlated (or anticorrelated), decreases the difference between the seep efficiencies of the DBM with $H=0.2$ and $H=0.8$ also decreases. This may be expected, since for large values of the cutoff a, there is only a small region in which the permeabilities are correlated (or anticorrelated), and for length scales $>>l$ the permeabilities become independent of H and are distributed randomly.

It might seem that quantifying the difference between the DBM and DLA model with quenched disorder and long-range correlations may also be possible through the differences between their fractal properties. However, as our results demonstrate, the interior of all the DBM aggregates that are obtained here is compact which, as discussed above, is due to the surface tension effects. Thus, only the *surface* of the aggregates might have fractal properties, if at all. On the other hand, the DLA patterns obtained here are more or less dendritic with small-scale randomness. They do not have any thick branches,

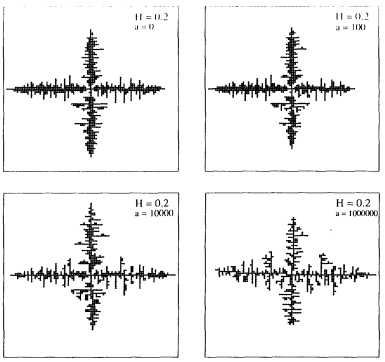

FIG. 9. The effect of the cutoff a on the growth patterns obtained with the DLA model, if the conductivities are anticorrelated.

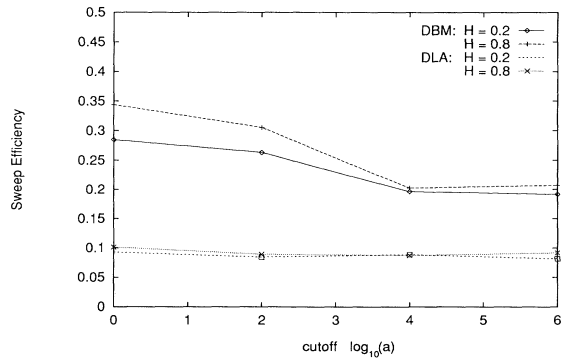

FIG. 11. The effect of the cutoff a on the sweep efficiency of the DBM and DLA model.

because surface tension effects are absent in the DLA model. Such patterns tend to be self-affine rather than self-similar, and their properties have been extensively studied [1]. Thus, we believe that the sweep efficiency is the most appropriate quantity for characterizing the difference between the DLA and the DBM aggregates obtained here.

V. SUMMARY

We investigated the effect of quenched disorder with long-range correlations, which are expected to be present in many systems of practical interest (especially in natural rock masses), on two growth phenomena, namely, DLA and the DBM. Even though our simulations were done in the limit of zero noise, i.e., the clusters were not grown stochastically, the results, especially those for the DBM, are quite different from those in the absence of long-range correlations. They indicate the dominant role of long-range correlations, and thus demonstrate that any realistic modeling of transport in rock must take into account the effect of such correlations. Elsewhere we have investigated [27] the effect of such long-range correlations on miscible displacements and viscous fingering in heterogeneous rocks. We have shown that, contrary to the popular belief, the viscosity contrast between the two fluids does not play any significant role, and the performance of the displacements is solely controlled by the heterogeneities with long-range correlations.

ACKNOWLEDGMENTS

We would like to thank Cristian Moukarzel for allowing us to use his efficient computer programs for generating the clusters. This work was carried out while one of us (M.S.) was visiting the HLRZ-KFA Supercomputer Center with support from the Alexander von Humboldt Foundation. He would like to thank the Foundation for financial support. One of us (K.B.L.) is grateful to the Danish Research Academy, and the Carlsberg Foundation for financial support that made his stay in Jülich possible. The first two authors would like to thank the HLRZ Center and its members for warm hospitality.

*Permanent address: Institute of Physics and Astronomy, Aarhus University, DK-8000 Aarhus C, Denmark.

†Present and permanent address: Department of Chemical Engineering, University of Southern California, Los Angeles, CA 90089-1211.

[1] P. Meakin, in *Phase Transitions and Critical Phenomena,* edited by C. Domb and J. L. Lebowitz (Academic, London, 1988), Vol. 12, p. 335.

[2] *Dynamics of Fractal Surfaces,* edited by F. Family and T. Vicsek (World Scientific, Singapore, 1991).

[3] T. Vicsek, *Fractal Growth Phenomena,* 2nd ed. (World Scientific, Singapore, 1992).

[4] *Fractals and Disordered Systems,* edited by A. Bunde and S. Havlin (Springer, Berlin, 1991).

[5] T. A. Hewett, Soc. Pet. Eng. New Orleans, LA (1986), paper 15386.

[6] T. A. Hewett and R. A. Behrens, Soc. Pet. Eng. Form. Eval. **5**, 217 (1990).

[7] For a review see M. Sahimi, Rev. Mod. Phys. (to be published).

[8] Y.-C. Zhang, J. Phys. (Paris) **51**, 2113 (1990).

[9] E. Medina, T. Hwa, M. Kardar, and Y.-C. Zhang, Phys. Rev. A **39**, 3053 (1989).

[10] A. Morgolina and H. E. Warriner, J. Stat. Phys. **60**, 809 (1990).

[11] J. G. Amar, P.-M. Lam, and F. Family, Phys. Rev. A **43**, 4548 (1991).

[12] C.-K. Peng, S. Havlin, M. Schwartz, and H. E. Stanley, Phys. Rev. A **44**, R2239 (1991).

[13] T. A. Witten and L. M. Sander, Phys. Rev. Lett. **47**, 1400 (1981).

[14] L. Niemeyer, L. Pietronero, and H. J. Wiesmann, Phys. Rev. Lett. **52**, 1033 (1984).

[15] B. B. Mandelbrot and J. W. Van Ness, SIAM Rev. **10**, 422 (1968).

[16] J. Feder, *Fractals* (Plenum, New York, 1988).

[17] H. O. Peitgen and D. Saupe, *The Science of Fractal Images* (Springer, New York, 1988).

[18] R.-S. Wu and K. Aki, Pure Appl. Geophys. **123**, 805 (1985).

[19] M. Sahimi, M. C. Robertson, and C. G. Sammis, Phys. Rev. Lett. **70**, 2186 (1993).

[20] L. Paterson, Phys. Rev. Lett. **52**, 1621 (1984).

[21] C. Tang, Phys. Rev. A **31**, 1977 (1985).

[22] J. Szép, J. Cresti, and J. Kertész, J. Phys. A **18**, L413 (1985).

[23] J. Nittmann and H. E. Stanley, Nature (London) **321**, 663 (1986).

[24] C. Moukarzel, Physica A **188**, 469 (1992).

[25] M. T. Batchelor and B. I. Henry, Phys. Rev. A **45**, 4180 (1992); Physica A **187**, 551 (1992).

[26] J.-D. Chen and D. Wilkinson, Phys. Rev. Lett. **55**, 1892 (1985).

[27] M. Sahimi and M. A. Knackstedt (unpublished).